

## The Interpretation of Kernels – An Overview

George K. Hung\* and Lawrence W. Stark†

\*Dept. of Biomedical Engineering  
Rutgers University  
P.O. Box 909  
Piscataway, NJ

†Neurology Unit  
Minor Hall  
University of California at Berkeley  
Berkeley, CA

(Received 2/20/91)

*The kernel identification method is a powerful technique for mathematically representing the dynamic behavior of a nonlinear system. This technique has been applied to a number of physical and physiological systems. An important development which has enhanced the usefulness of the kernel method has been the interpretation of the internal structure of a system by examining the shapes of the higher-degree kernels. Examples of various nonlinear models with known structure are illustrated to show a repertoire of kernel shapes. Variations in parameters of these models result in well-defined changes in the shapes of the kernels. Also, examples are shown of kernels obtained from physiological systems to demonstrate how examination of kernel shapes can lead to accurate predictions of the dynamic behavior of the physiological system. Finally, limitations of the applicable range of the kernel identification method are discussed.*

**Keywords**—*Interpretation, Kernel shapes, Models, Physiological systems, Usefulness, Limitations.*

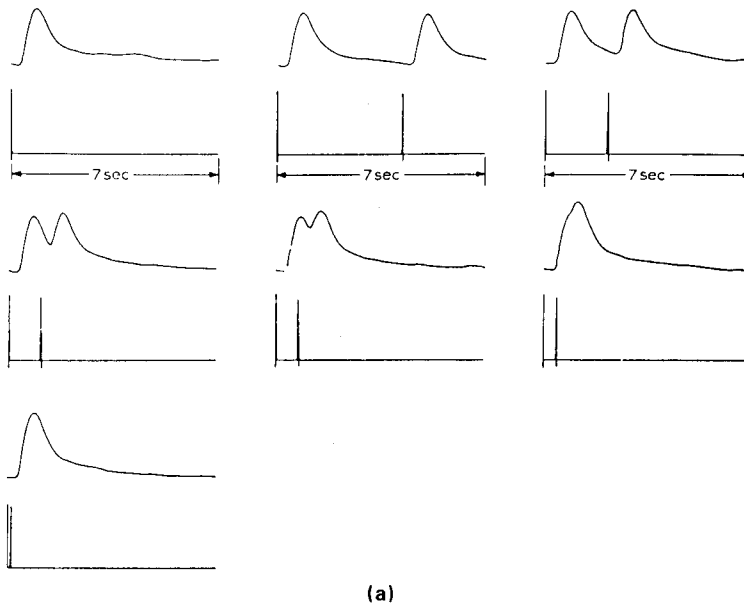
The kernel identification method is a mathematical technique used for representing a nonlinear dynamic system in a manner analogous to that of a polynomial expansion for a static nonlinearity. Volterra (1) was the first to formalize the mathematical expression for an integral series by means of higher degree kernels. Wiener (2) showed how this series could be orthogonalized and how a circuit might be constructed to represent the kernels. Over the next three decades following Wiener, there has been a great deal of research done on the efficient computation of kernels of physical systems. In addition, a number of investigators have contributed to the theory and application of the kernel identification method. For some detailed reviews, see (3-6).

---

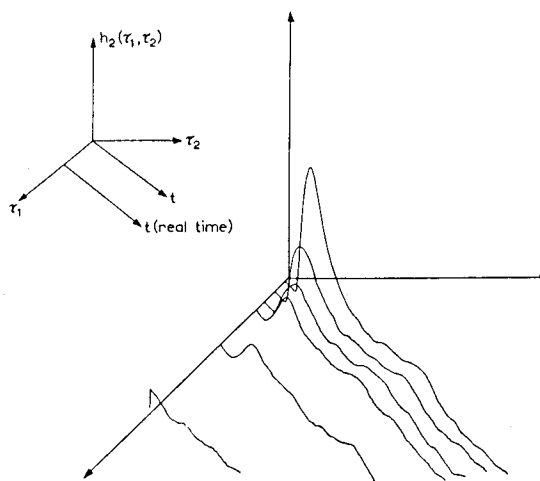
*Acknowledgment*—Partial support was provided by a Rutgers University Research Council Grant to G.K.H.

Address correspondence to George K. Hung, Department of Biomedical Engineering, Rutgers University, P.O. Box 909, Piscataway, NJ 08854.

In a number of systems, most of the nonlinearity is contained in the 2nd-degree kernels. For such systems, the double-pulse approach is particularly suitable since the experimental and computational requirements are relatively simple. Sandberg and Stark (7) obtained 2nd-degree kernels of the human pupillary system by using the double-pulse approach (Fig. 1). However, for systems containing significantly higher-



(a)



(b)

**FIGURE 1.** (a) Double-pulse light stimulus of the human pupillary system. (b) Associated 2nd-degree kernels derived from double-pulse experiments (7).

degree kernel contributions, other approaches are needed. For example, if the shape of the system responses are similar to well-known functions, such as the Laguerre and Legendre functions, an orthogonal basis-function approach could be used. Watanabe and Stark (8) obtained a hyperplane of the 3rd-degree kernels by using this approach (Fig. 2). On the other hand, for the general system, standard techniques such as the cross-correlation method developed by Lee and Schetzen (9), and the frequency domain method described by Brillinger (10), have been used. For example, Sandberg and Stark (7) obtained the 1st- and 2nd-degree kernels of the human pupillary system by using the cross-correlation method (Fig. 3).

A significant development in the application of the kernel identification technique has been the interpretation of the internal structure of systems by examining the shape of the higher-degree kernels (11–13). Some examples of the expected kernel shapes for various model configurations are shown in Table 1 (11). A model consisting of two pre-multiplier linear elements followed by a linear element (11) has been examined in detail (Fig. 4a). The simulation results (Fig. 4b) illustrate that the smaller pre-multiplier time constant controls decay of the 2nd-degree kernels parallel to the main diagonal, whereas the larger pre-multiplier time constant controls decay in the off-diagonal direction. Also, the post-multiplier time constant smears the kernels parallel to the main diagonal.

The human pupillary system has been studied to determine the relationship between its well-known nonlinear dynamic behavior and the shape of the kernels. Pu-

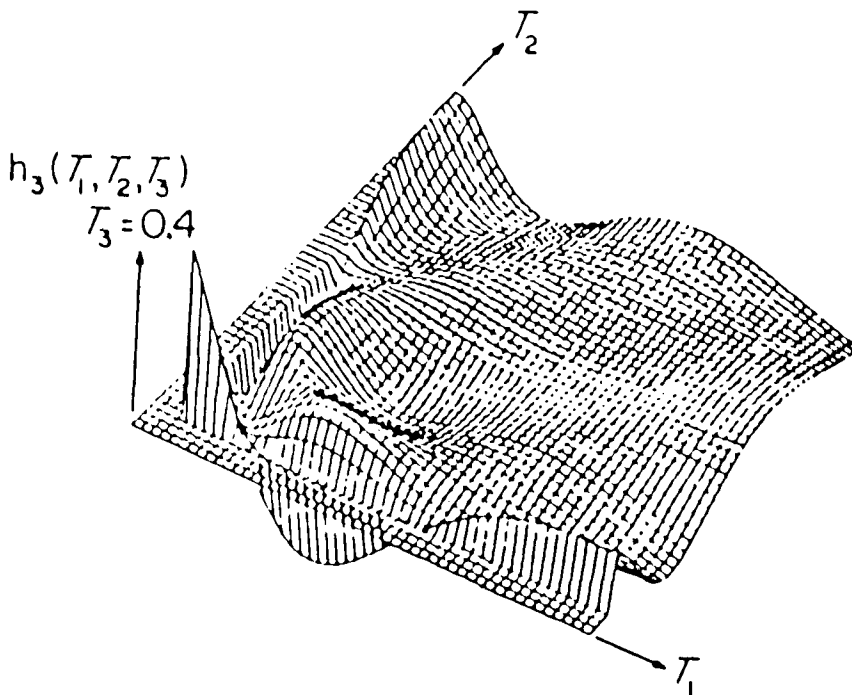


FIGURE 2. 3rd-degree kernels of the human pupillary system; cross section at hyperplane  $T_3 = 0.4$  sec. (8).

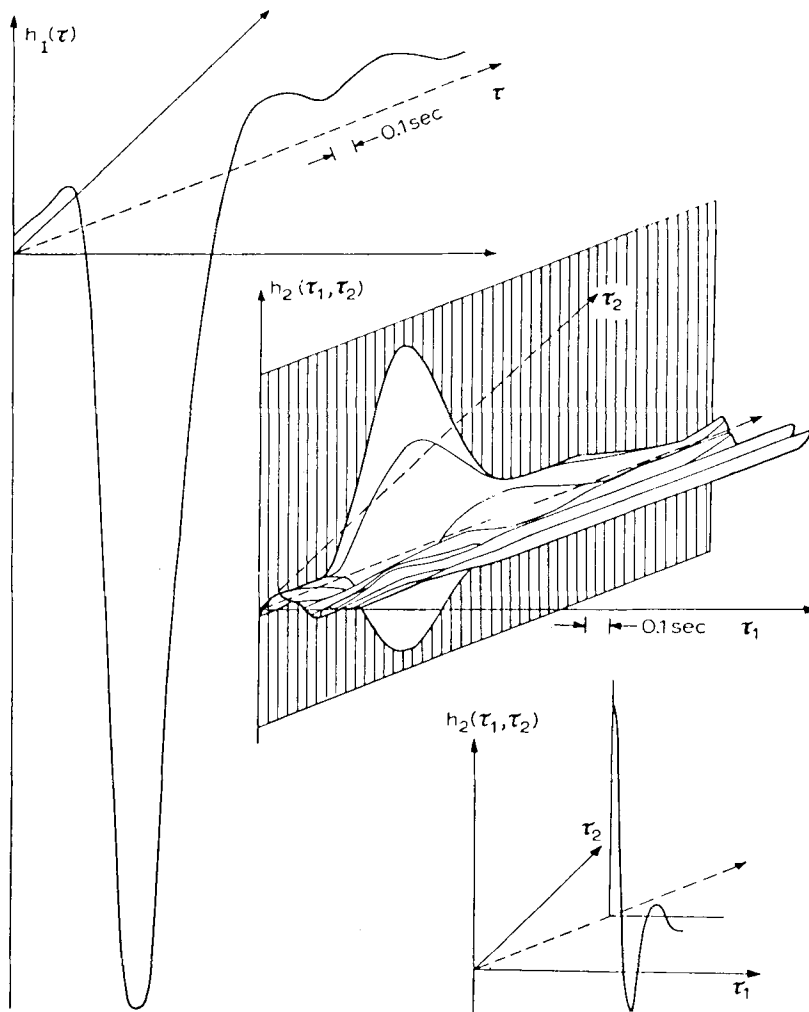


FIGURE 3. 1st- and 2nd-degree kernels of the human pupillary system obtained by means of the cross-correlation method (7).

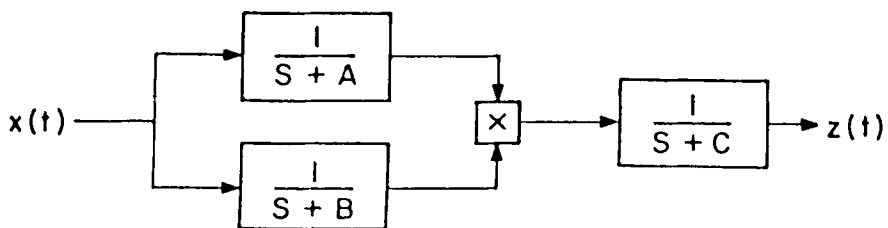


FIGURE 4(a). Model consisting of pre-multiplier linear elements with time constants  $1/A$  and  $1/B$ , and post-multiplier element with time constant  $(1/C)$ .

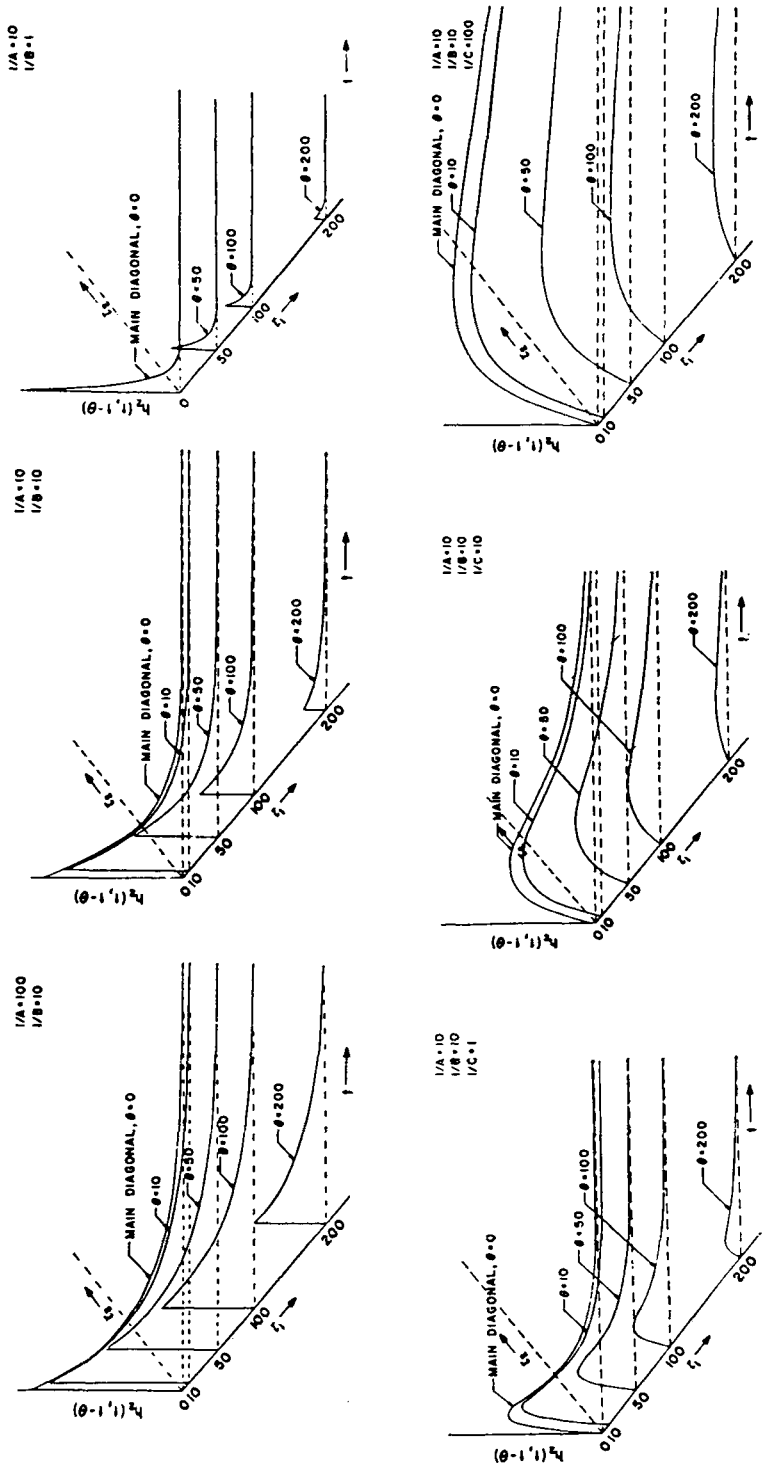


FIGURE 4(b). Quadratic kernels obtained by means of bi-impulse simulation. Top row (without post-[X] TC) shows smaller Wiener-type pre-[X] TC (1/B) controls decay parallel to the main diagonal. It also shows larger pre-[X] TC (1/A) controls off-diagonal decay. Bottom row shows Hammerstein-type post-[X] TC (1/C) smears mostly parallel to main diagonal (1 1).

TABLE 1. Examples of quadratic dynamic systems and their kernel characteristics.

	DIAGRAM	$h_2(t_1, t_2)$	SYMMETRY	CHARACTERISTICS OF $h_2$
a.	<p>NO DYNAMICS</p>	$\delta(t_1) \delta(t_2)$	YES	
b.	<p>HAMMERSTEIN MODEL</p>	$h_c(t_1) \delta(t_1 - t_2)$ DIAGONAL $t_1 = t_2$ ONLY	YES	
c.	<p>WIENER MODEL</p>	$h_o(t_1) h_o(t_2)$ $\frac{h_2(t_1, c_1)}{h_2(t_1, c_2)} = \text{CONSTANT}$	YES	
d.		$h_o(t_1) h_b(t_2)$	1	
e.		$\int h_o(t_1 - \zeta) h_b(t_2 - \zeta) h_c(\zeta) d\zeta$	1	
f.		$\int h_o(t_1 - \zeta) h_b(t_2 - \zeta) h_c(\zeta) d\zeta$	IFF $h_o = h_b$	
	ONE INPUT			
	TWO INPUTS			

pupillary response to on-step of light consists of a rapid constriction with overshoot, followed by redilation, whereas the response to off-step of light shows only a slow dilatation. Thus, the pupillary system exhibits asymmetry to on and off stimuli. For the pupillary kernel model, the pupillary 1st- and 2nd-degree main-diagonal kernels were examined in terms of their signs. It can be shown that the 1st-degree kernels are analogous to the linear term, whereas the 2nd-degree main-diagonal kernels are analogous to the quadratic term, in a power series expansion. Thus, it is expected that the 1st-degree kernels should show asymmetric responses to on- and off-steps of input, whereas the 2nd-degree main-diagonal kernels should show symmetric responses to on- and off-step inputs. If the 1st- and 2nd-degree kernels are of the same sign, then in response to an off-step input, the contribution from the main-diagonal of the 2nd-degree kernel would partly cancel the negative response contribution from the 1st-degree kernel. Therefore, the total system response should show an asymmetry to on and off stimuli. Indeed, consistent with the above, experimentally determined 1st- and 2nd-degree main-diagonal kernels of the pupillary system have been found to exhibit the same sign (14).

The overshoot following pupillary constriction in response to a step of light input is called pupillary escape. It was proposed that larger amplitude 2nd-degree off-diagonal kernels corresponded to larger amounts of escape in the system response (15). To quantify this behavior, a heuristic model, consisting of linear and quadratic

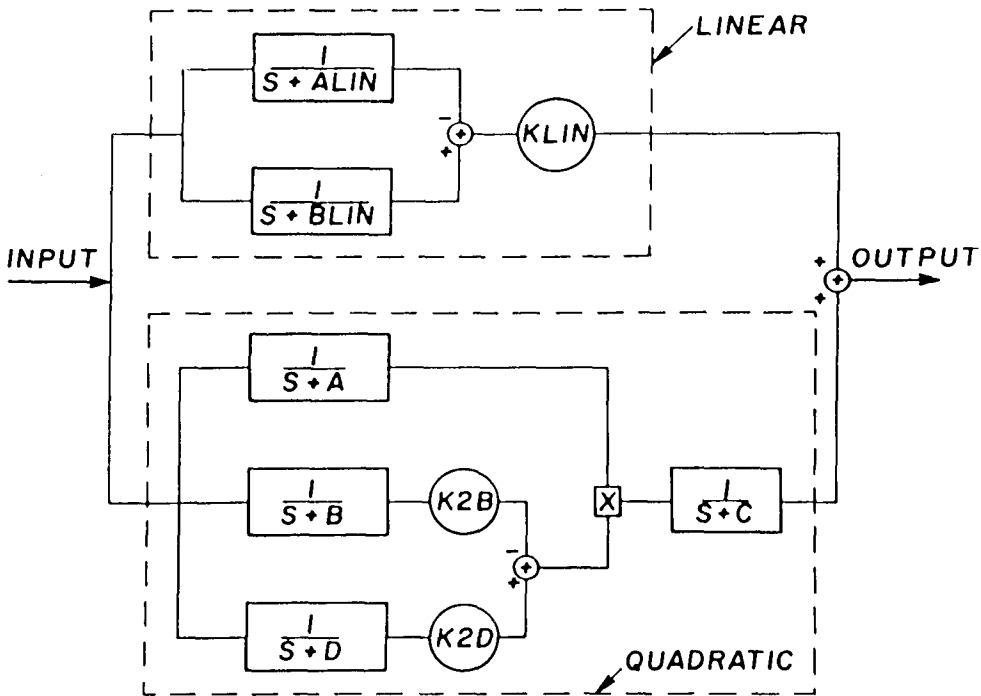


FIGURE 5. Heuristic model used in the simulation of the pupillary escape phenomenon. It contains linear and quadratic sections, each composed of combinations of simple linear elements. Reciprocal time constants:  $A = 2.0$ ,  $B = 4.0$ ,  $C = 2.5$ ,  $D = 1.5$ ,  $ALIN = 2.0$ ,  $BLIN = 35.0$ . Gain  $KLIN = 35.0$ . Gains  $K2B$  and  $K2D$  were varied to produce different amounts of escape (15).

sections, was developed. This allowed for the control of varying amounts of escape in the model response (Fig. 5). Simulation results showed that, indeed, the off-diagonal kernel magnitude increased as the amount of escape increased (Fig. 6).

A novel approach for obtaining the nonlinear open-loop transfer function of the

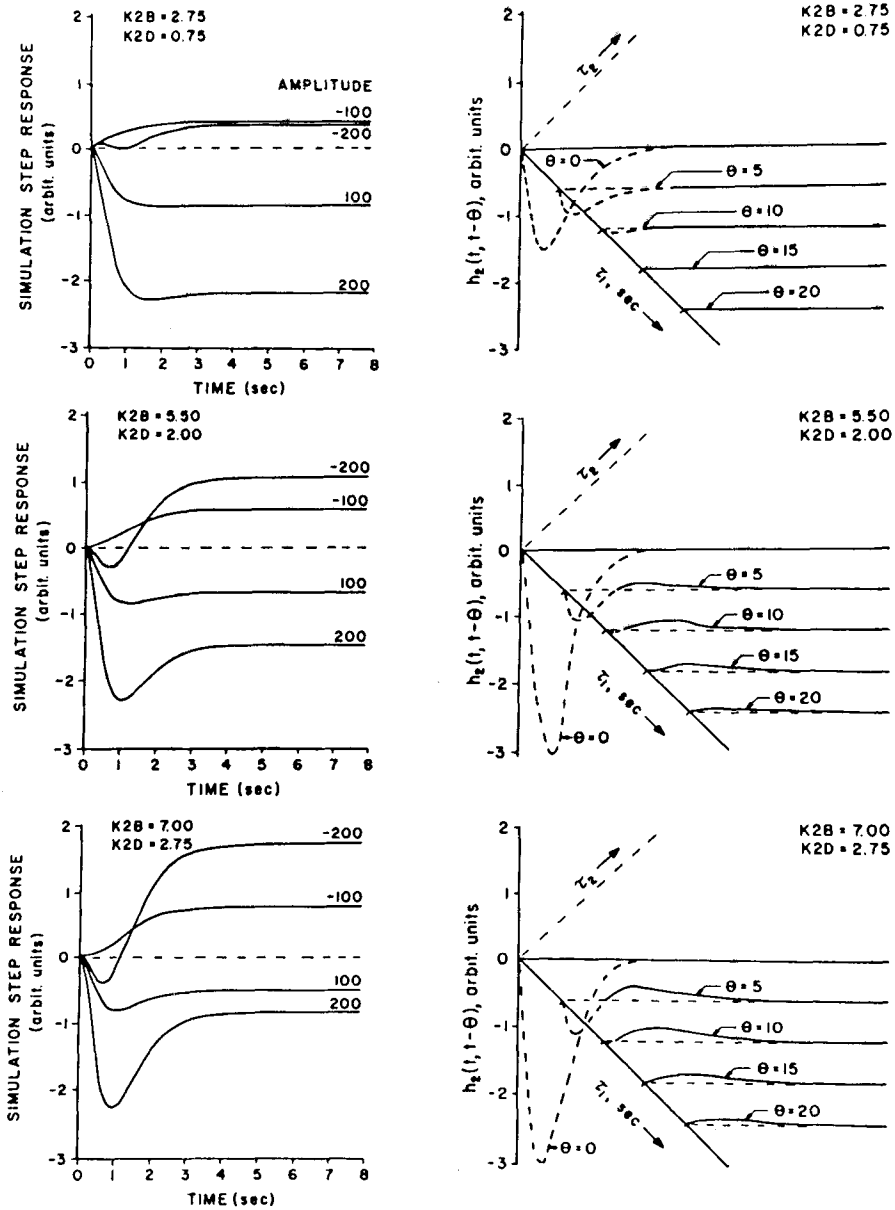


FIGURE 6. Step responses and 2nd-degree kernels of the heuristic model (Fig. 5). Left column from top to bottom shows increase in escape as the parameters  $K2B$  and  $K2D$  were varied. Right column shows corresponding increase in the magnitude of off-diagonal kernels (15).



human operator was developed by Hung (16). In a typical experiment, the human operator controlled a joystick which in turn drove a simulated plant (either  $K$ ,  $K/s$ , or  $K/s^2$ ). The error between a random input signal (of various bandwidths) and the plant output were displayed on a screen. The operator's task was to minimize this error. The paradigm was repeated for random signals of various bandwidths over a number of experimental sessions. Then, unknown to the subject, in certain sessions, the pre-recorded error signal itself was presented to him. Thus, the subject was operating under open-loop conditions. At the end of all the experiments, the subjects reported that they were unaware of the open-loop conditions. The kernels were calculated using the open-loop experimental data. A mathematical kernel representation of the human operator under open-loop conditions is shown in Fig. 7. Table 2 lists the (rms) of the difference between experimental and kernel model responses for different sums of 1st-, 2nd-, and 3rd-degree kernels. It was noted that in a number of cases the rms increased as higher-degree kernel contributions were added. One possible explanation is that the human operator is essentially linear and that additional nonlinear contributions were near the noise level. Another explanation is that the plant filtered out much of the nonlinear contributions from the human operator during the closed-loop experiments, leaving mainly the linear contribution in the error signal.

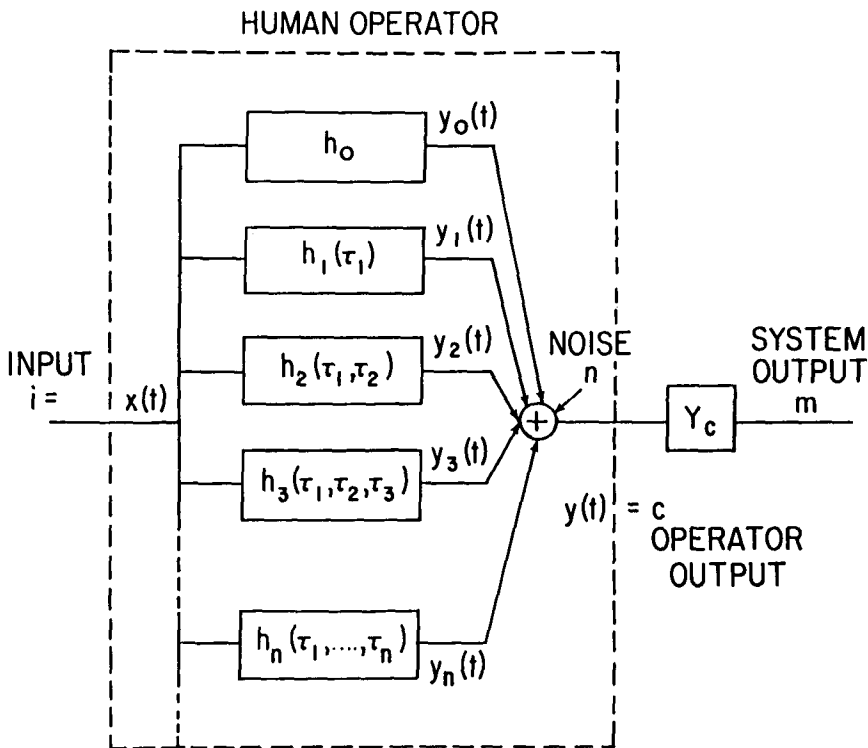


FIGURE 7. Block diagram of open-loop compensatory system showing human operator as a subsystem represented mathematically by higher degree kernel terms (16).

**TABLE 2. RMS difference between experimental response and response of (sum of degrees) kernel models for different plants and input bandwidths. Values in equivalent visual angle of manual control movements, in degrees [16].**

Type of Controlled Plant	Input Bandwidth (rad/sec)	Degree Model		
		1	1 & 2	1, 2 & 3
K	4.17	0.099	0.098	0.122
	10.9	0.141	0.136	0.158
K/S	2.58	0.347	0.257	0.261
	4.17	0.178	0.166	0.183
	10.9	0.291	0.294	0.346
K/S <sup>2</sup>	2.58	0.198	0.215	0.204
	6.75	0.231	0.232	0.279

The kernel identification method is a powerful technique for mathematically representing nonlinear systems. However, this technique is not a panacea for treating all nonlinearities, and indeed, must be used with care. We wish to point out two important limitations. First, the kernels are meaningful only at the dc level and at the ac amplitude of the applied signal. In other words, it may require an "army" of kernels (17) to represent a system at all practical dc and ac levels (12). Second, the kernel method may not be suitable for sharply nonlinear systems, but instead is more useful for weakly nonlinear systems, especially if only lower-degree kernels can be calculated accurately (18).

## REFERENCES

- Volterra, V. *Theory of functionals*. Glasgow: Blackie and Sons; 1930.
- Wiener, N. *Nonlinear problems in random theory*. New York: Wiley; 1958.
- Hung, G.; Stark, L. The kernel identification method (1910-1977)—Review of theory, calculation, application, and interpretation. *Math. Biosciences* 37:135-190; 1977.
- Marmarelis, P.Z.; Marmarelis, V.Z. *Analysis of physiological systems: The white noise approach*. New York: Plenum Press; 1978.
- Schetzen, M. *The Volterra and Wiener theories of nonlinear systems*. New York: Wiley; 1980.
- Rugh, W.J. *Nonlinear system theory: The Volterra-Wiener approach*. Baltimore: Johns Hopkins University Press; 1981.
- Sandberg, A.; Stark, L. Wiener G-function analysis as an approach to nonlinear characteristics of human pupil light reflex. *Brain Res.* 11:194-211; 1968.
- Watanabe, A.; Stark, L. Kernel method for nonlinear analysis: Identification of a biological control system. *Math. Biosci.* 27:99-108; 1975.
- Lee, Y.W.; Schetzen, M. Measurement of the Wiener kernels of a nonlinear system by cross-correlation. *Int. J. Control* 2:237-254; 1965.
- Brillinger, D.R. The identification of polynomial systems by means of higher order spectra. *J. Sound Vib.* 12:301-313; 1970.
- Hung, G.; Stark, L.; Eykhoff, P. On the interpretation of kernels. I. Computer simulation of responses to impulse pairs. *Annals of Biomedical Engineering* 5:130-143; 1977.

12. Krenz, W.; Stark, L. Interpretation of kernels of functional expansions. *Advanced Methods of Physiological Systems Modelling* 1:241–257; 1986.
13. Chen, H.W.; Jacobson, L.D.; Gaska, J.P. Structural classification of multi-input nonlinear systems. *Biol. Cyber.* 63:341–357; 1990.
14. Hung, G.; Brillinger, D.R.; Stark, L. Interpretation of kernels. II. Same-signed 1st- and 2nd-degree (main-diagonal) kernels of the human pupillary system. *Math. Biosci.* 46:159–187; 1979.
15. Hung, G.; Stark, L. Interpretation of kernels. III. Positive off-diagonal kernels as correlates of the dynamic process of pupillary escape. *Math. Biosci.* 46:189–203; 1979.
16. Hung, G. The separation of human operator nonlinearities and variability noise by means of “open-loop” compensatory tracking: Higher degree kernels as estimates of nonlinear contributions. NASA Ames Res. Center (internal communication); 1978.
17. Marmarelis, P.; Naka, K. White noise analysis of a neuron chain: An application of the Wiener theory. *Science* 175:1276–1278; 1972.
18. Wiener, D.; Spina, J. *Sinusoidal analysis and modeling of weakly nonlinear circuits*. Van Nostrand Reinhold Co.; 1980.